5.2.3 Ruthenium Metal Agglomeration Phenomenon Results Summary

5.2.3.1 Effect of Particle Size on Ruthenium Metal Agglomeration

Catalyst 4966-72 (1.05% Ru on Al_2O_3) with 0.8 nm ruthenium particles and with H_2:Ru ratio of 1.1, Catalyst 4956-86 (0.85% Ru on Al_2O_3) with <2 nm ruthenium particles and with H_2:Ru ratio of 0.85, Catalyst 4956-101 (0.86% Ru on Al_2O_3) with $\leq$2-4 nm and with H_2:Ru ratio of 0.59, Catalyst 4966-96-1 (1.12% Ru on Al_2O_3) with 3-7 nm ruthenium particles and with H_2:Ru ratio of 0.50 and Catalyst 4956-76 (0.93% Ru on Al_2O_3) with 4-6 nm ruthenium particles and with H_2:Ru = 0.29 were tested at 208°C and 35 atm. The H_2:CO feed ratio was 0.9 for Catalysts 4956-86, 4956-101 and 4956-76 in Runs 16, 17 and 15, respectively, and 2.0 for Catalysts 4966-72 and 4966-96-1 in Runs 25 and 24, respectively. Later in Run 24, the test with Catalyst 4966-96-1 was extended to cover performance at a higher temperature of 225°C and/or at a higher pressure of 100 atm.

During tests with Catalysts 4966-72, 4956-86 and 4956-101 with smaller than 4 nm ruthenium particles, ruthenium carbonyl was detected at the reactor outlet in the product receivers, substantial fraction of the ruthenium was lost from the catalysts and extensive ruthenium metal agglomeration occurred. Despite the seemingly severe conditions in the tests with Catalyst 4966-96-1 (3-7 nm ruthenium particles), agglomeration was very mild and appeared to effect only the 3-4 nm ruthenium particles which were present in the fresh catalyst but not in the used catalyst. It appeared that 3-4 nm ruthenium particles in Catalyst 4966-96-1 agglomerated to the 4-7 nm size range. There was no noticeable increase in the fraction of ruthenium particles in the 7-10 nm size range. Ruthenium carbonyl was not observed at the reactor outlet, ruthenium was not lost and ruthenium agglomeration did not occur with Catalyst 4956-76 having 4-6 nm ruthenium particles [74].

The extent of ruthenium metal agglomeration was suppressed, but not totally eliminated, apparently by using higher H_2:CO feed ratio in Run 18 relative to Run 16 with highly dispersed ruthenium Catalysts 4966-72 and 4956-86, respectively.

The steam partial pressure did not have a major effect on ruthenium metal agglomeration. The extent of ruthenium agglomeration was not reduced by minimizing the steam partial pressure in Run 25 with highly dispersed ruthenium Catalyst 4966-72. During that test, more than 90% of the water made in the Fischer-Tropsch synthesis reaction was converted to H_2 via the water gas shift reaction.

Ruthenium metal agglomeration with smaller than 4 nm ruthenium particles over alumina is consistent with the results reported by Kellner and Bell, as described in Section 2.2.4 [55].

Since ruthenium carbonyl formation and overall ruthenium loss accompanied ruthenium agglomeration, ruthenium agglomeration is believed to occur via the formation of the volatile ruthenium carbonyl species. Overall ruthenium loss from 3-4 nm ruthenium particles on Al_2O_3 via the formation of the volatile ruthenium carbonyl species was also reported by Goodwin, *et al.*, who suggested that the extent of carbonyl formation may be dependent on catalyst characteristics including metal particle size [75].

Ruthenium carbonyl formation probably requires undissociated CO. Dissociation of CO might be expected to be suppressed over small ruthenium particles since it probably requires a large ensemble of atoms [76]. Accordingly, ruthenium carbonyl formation may be enhanced over small ruthenium particles and cause ruthenium agglomeration. Multiple CO adsorption per ruthenium atom as Della Betta observed using IR [77] with small ruthenium particles also should help the formation of ruthenium carbonyl.

5.2.3.2 Effect of Support on Ruthenium Metal Agglomeration

5.2.3.2.1 Y-Zeolite vs. Alumina

The significance of Y-zeolite *vs.* alumina support in ruthenium metal agglomeration was investigated by comparing Catalyst 4966-114 (6.3% Ru on Y-zeolite) and Catalyst 4966-76 (0.84% Ru on Al_2O_3). The ruthenium compounds that were used and the preparation procedures were different with these two catalysts (Table 5-41). Nevertheless, a nearest-neighbor coordination number of 8.4 was calculated for both catalysts by EXAFS, which corresponds to a ruthenium particle size equal to 1.5 nm (Figure 5-256). From the magnitude of Fourier transform peaks from more distant shells the alumina-supported catalyst seemed to have some ruthenium particles larger than 1.5 nm, while the zeolite-supported catalyst did not. These two catalysts were tested under identical conditions 1.5 H_2:CO feed ratio, 200°C and 14 atm in Runs 20 and 28. The ruthenium in the alumina-supported catalyst partly agglomerated in 12 hours, while there was no noticeable ruthenium agglomeration with the zeolite-supported catalyst after 28 hours of testing at comparable conversion levels (Table 5-41).

5.2.3.2.2 Titania vs. Alumina

The significance of titania *vs.* alumina support in ruthenium metal agglomeration was investigated by comparing Catalyst 5345-61 (0.93% Ru on TiO_2) and Catalyst 4966-72 (1.05% Ru on Al_2O_3). Identical preparation procedures were used, except the titania-supported catalyst was treated with H_2 at 600°C before the test (Table 5-42). According to STEM examination, both catalysts consisted of ruthenium particles which were smaller than 2 nm. These two catalysts were tested at $2H_2$:1CO feed ratio, 208°C at inlet and 35 atm for 12 hours in Runs 30 and 25, respectively.

TABLE 5-41

CONTROL OF RUTHENIUM METAL AGGLOMERATION ON Y-TYPE ZEOLITE

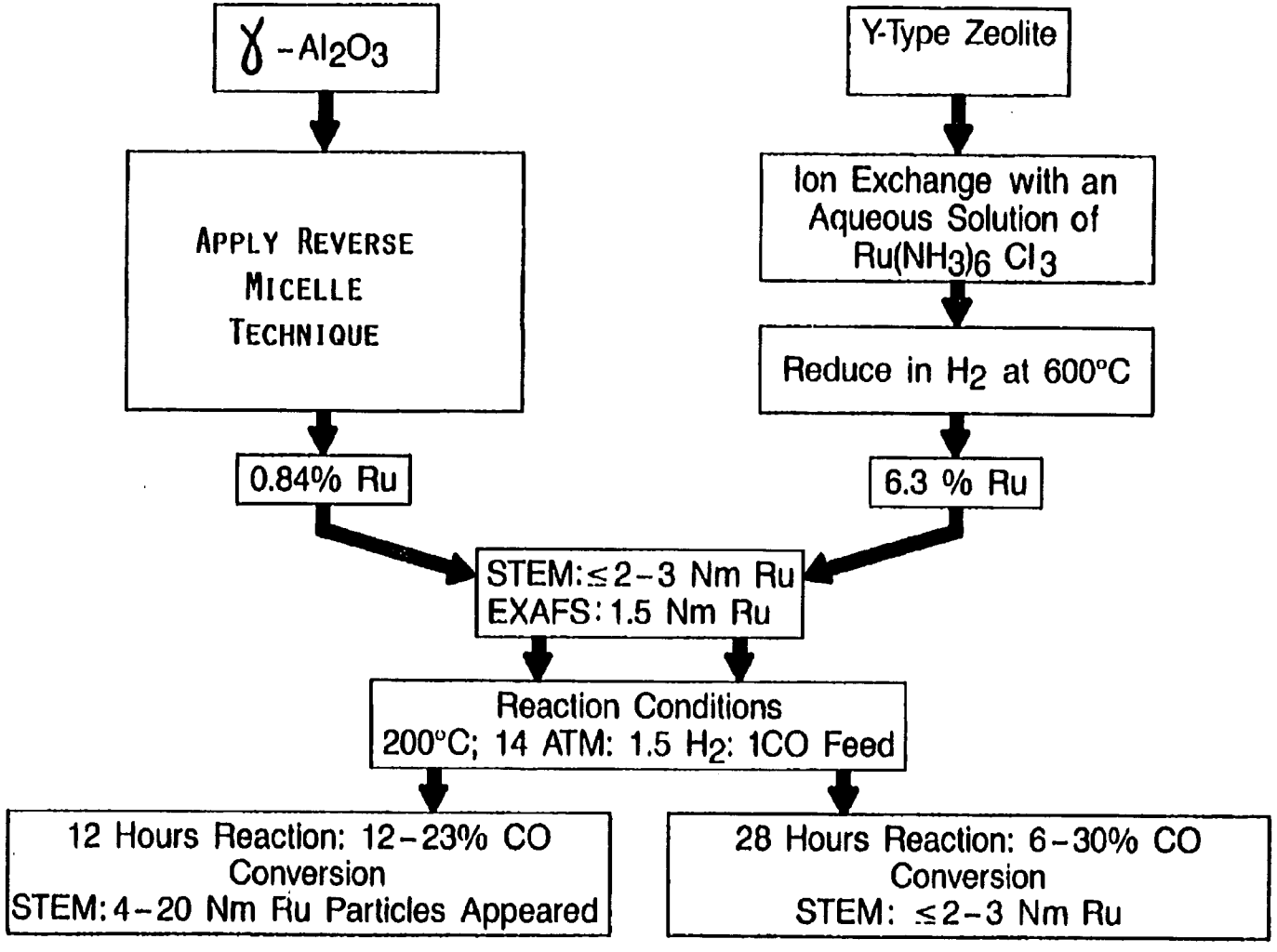

Figure 5-256

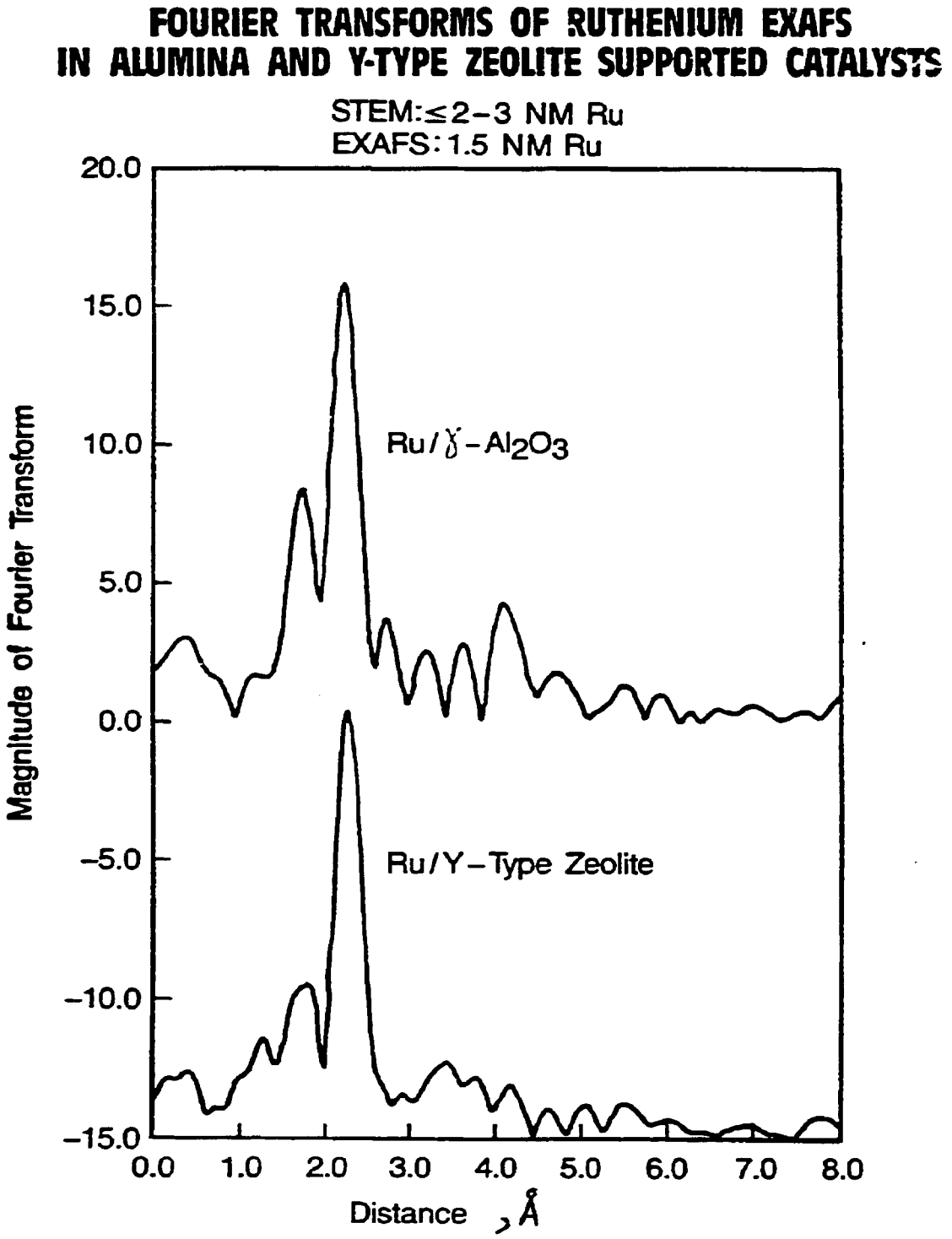
FOURIER TRANSFORMS OF RUTHENIUM EXAFS
IN ALUMINA AND Y-TYPE ZEOLITE SUPPORTED CATALYSTS
STEM:≤2-3 NM Ru
EXAFS: 1.5 NM Ru
Ru/γ-Al2O3
Ru/Y-Type Zeolite
Magnitude of Fourier Transform
Distance, Å
20.0
15.0
10.0
5.0
0.0
-5.0
-10.0
-15.0
0.0
1.0
2.0
3.0
4.0
5.0
6.0
7.0
8.0

Table 5-42. **CONTROL OF RUTHENIUM METAL AGGLOMERATION ON TITANIA**

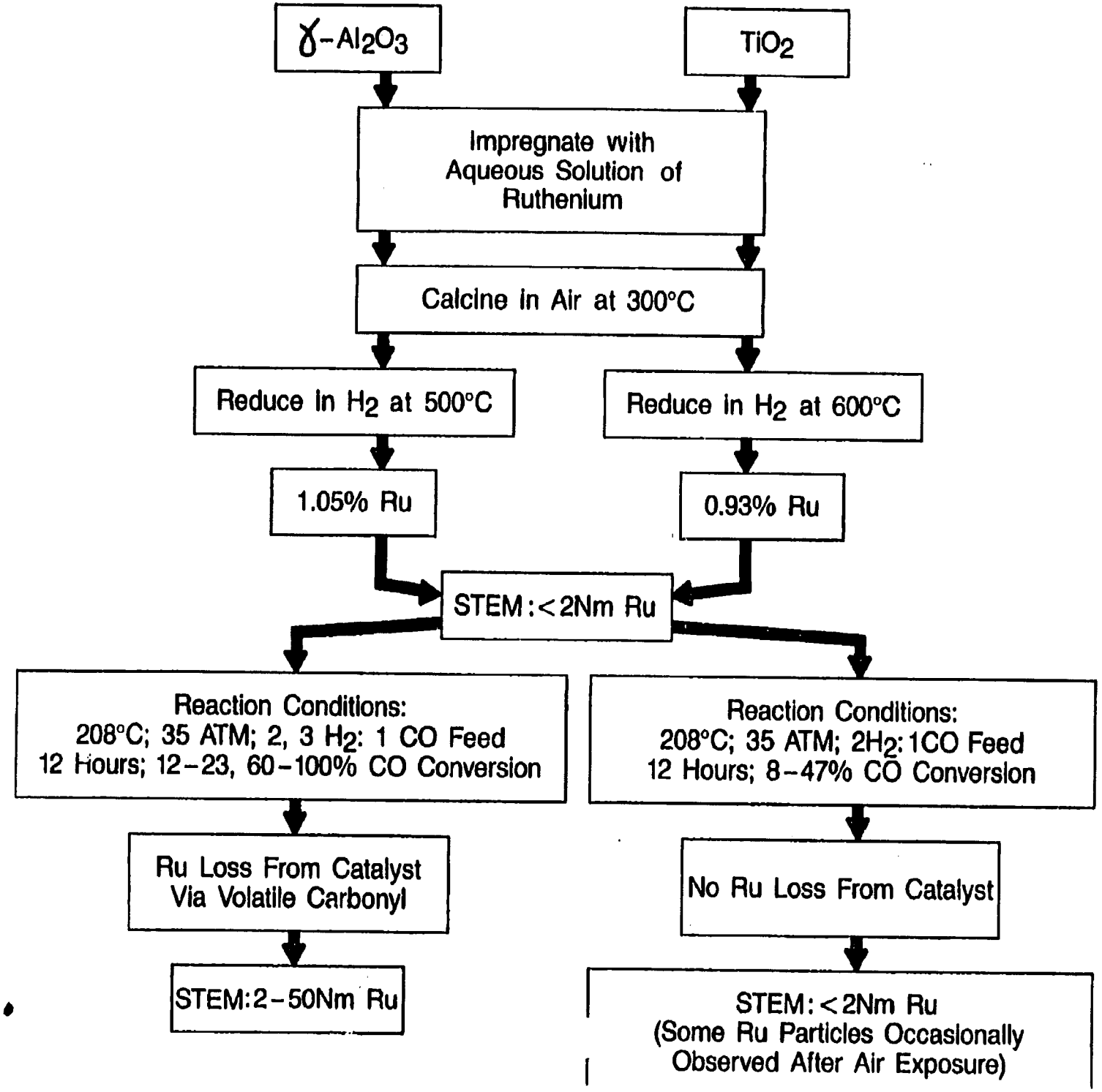

There was ruthenium loss in the form of volatile carbonyl from the alumina-supported catalyst, accompanied by ruthenium agglomeration. Ruthenium was not lost from the titania-supported catalyst and there was no noticeable rutheium agglomeration during the first STEM examination. Some 1-5 nm ruthenium particles were observed during reexamination of the same STEM sample four months later. The STEM sample was exposed to air during the four-month period.

Differences in the extent of ruthenium metal agglomeration between different catalysts with similar size ruthenium particles may be possibly attributed to differences in the nature of support. However, at this stage, the possible effect of catalyst preparation procedure differences on ruthenium agglomeration cannot be ruled out.

5.2.4 Hydrocarbon Cutoff Hypothesis Investigation Summary

The product distributions were Anderson-Schulz-Flory with increasing chain growth probability at higher carbon number and with no cutoff, at least up to C_{160}, with $\leq$2-4 nm ruthenium particles on alumina in Run 20, with smaller than 20Å ruthenium particles on titania in Run 30 and with 1.5 nm ruthenium particles on Y-zeolite in Run 28. These results indicate that cutoff was not effected by limiting the size of the active metal particle to the range investigated in this work.

It is conceivable that a very large number of literature reports of hydrocarbon cutoff are not valid since these reports don't mention analysis of used catalysts for condensed hydrocarbons.

5.2.5 Ruthenium Metal Particle Size Effects in Fischer-Tropsch Synthesis

5.2.5.1 Activity Effect

Two sets of results, under two different sets of conditions, were obtained with five alumina-supported catalysts, 4966-72, 4956-86, 4956-101, 4966-96-1, and

4956-76 in Runs 32, 16, 17, 33 and 15, respectively. The test conditions and the apparent initial turnover frequency for these catalysts are shown in Table 5-43 as a function of the H_2:Ru ratio. The turnover frequency here is defined

Table 5-43

Variation of Initial Activity with Ruthenium Particle Size on Alumina (35 atm)

Catalyst	H_2:Ru	Run	Hours	GHSV	T, °C (Inlet)	T, °C (Maximum)	H_2:CO Feed Ratio	CO Conv. %	TOF*
4956-86	0.85	16	7	70	208	210	0.9	15	0.0024
4956-101	0.59	17	7	70	208	212	0.9	25	0.0073
4956-76	0.29	15	7	70	208	215	0.9	42	0.023
4966-72	1.1	32	27	65	225	232	2.0	66	0.0089
4966-96-1	0.50	33	36	140	225	233	2.0	73	0.026

*Initial Apparent Turnover Frequencies
(Moles CO Converted/Sec - Moles Ru x H_2:Ru)

as moles CO converted per second per mole exposed ruthenium. The turnover frequency is qualified as apparent because the fractional dispersion of ruthenium was assumed to be equal to the H_2:Ru ratio. For the first set of results, activity reported here corresponds to the CO conversions measured at 7 hours on stream in Runs 16, 17 and 15 at the same space velocity. Initial data were compared in order to minimize the effects of ruthenium metal agglomeration. For the second set of results, activity reported here corresponds to approximately the same CO conversion obtained at two different space velocities in Runs 32 and 33.

A 10-fold decrease in the apparent turnover frequency was observed when the H_2:Ru ratio was increased from 0.29 to 0.85 at 208°C inlet temperature and at a H_2:CO feed ratio of 1.09. Results at 225°C and $2H_2$:1CO ratio also showed a decrease in the turnover frequency with increase in the H_2:Ru ratio. Most of the differences in CO turnover frequencies were caused by differences in hydrocarbon synthesis activities.

However, it is important to point out that with larger ruthenium particles higher activity caused higher temperatures in the catalyst beds, which in turn

amplified the activity differences between catalysts of different particle sizes. However, increase in conversion with increase in ruthenium particle size caused the H_2:CO ratio in the catalyst bed to decrease below the value in the feed and, therefore, have an adverse effect on activity. Because of these factors, the turnover frequency results reported here should be used to show trends between catalysts of different particle sizes and not treated in an absolute manner.

5.2.5.2 Selectivity Effects

5.2.5.2.1 Water Gas Shift Reaction

Catalysts 4956-86 (Run 16), 4956-101 (Run 17), and 4956-76 (Run 15), for which the test conditions were described in Table 5-43, are compared in Figure 5-257. Here, the selectivity of conversion of CO to CO_2 is plotted versus the CO conversion and versus time on stream. The ratio of moles H_2 consumed to moles CO consumed decreased to a value lower than 2 as the selectivity to CO_2 increased. As it is discussed in section 5.2.1.1.1 and in the appendix, analysis of the CO/H_2 reaction system in this work indicates that the water gas shift reaction, and not the Boudouard reaction ($2CO \rightarrow CO_2+C$) was most likely to be the source of CO_2. Accordingly, throughout this work CO_2 formation is tentatively attributed to the water gas shift reaction.

Catalyst 4956-76 with 4-6 nm ruthenium particles and Catalyst 4956-101 with 2-4 nm or smaller ruthenium particles apparently showed water gas shift activity only during the first few hours of testing. The highest selectivity to the water gas shift reaction was maintained for over 75 hours with Catalyst 4956-86 having the smallest ruthenium particle size (smaller than 2 nm), at converison levels comparable to those obtained with Catalysts 4956-101 and 4956-76.

Selectivities of CO conversion to CO_2 obtained in Runs 25 and 24 with Catalysts 4966-72 and 4966-96-1 having different size ruthenium particles, along with the test conditions, are summarized in Table 5-44.

Figure 5-257. CO_2 Selectivities with Catalysts Having Different Size Ruthenium Particles in Runs 16, 17 and 15 (H_2:CO Feed Ratio = 0.9, 208°C at Inlet, 35 atm)

	Catalyst	Run	H_2:Ru	Ru, nm (STEM)
◇	4956-86	16	0.85	<2
□	4956-101	17	0.59	≤2-4
○	4956-76	15	0.29	4-6

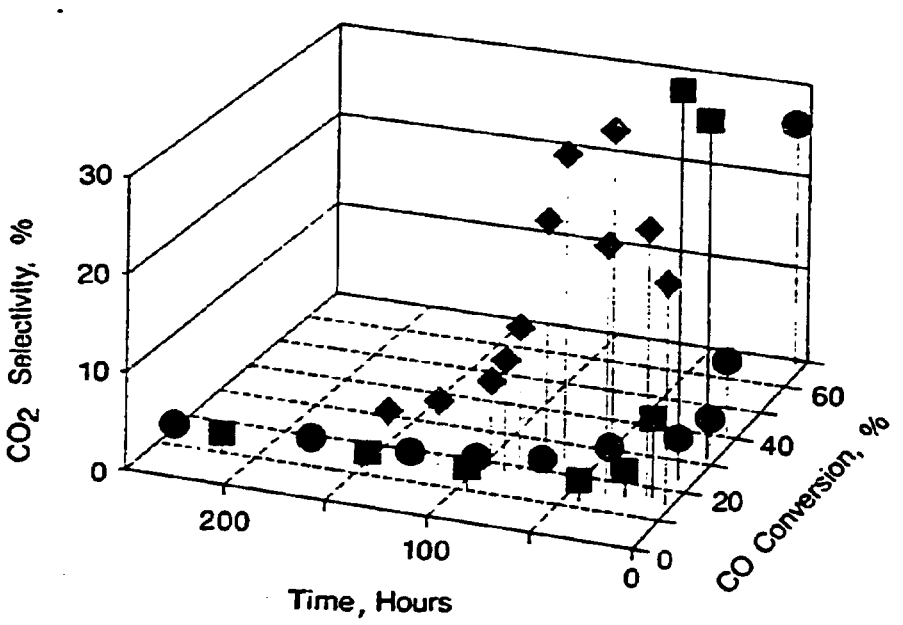

Table 5-44

Variation of Water Gas Shift Activity with Ruthenium Particle Size on Alumir
(H_2:CO Feed Ratio = 2.0, 208°C at Inlet, 35 atm)

.alyst	Run	Hours on Stream	Initial Ru Partricle Size	H_2:Ru	CO_2 Selectivity, %	H_2:CO Usage Ra
4966-72	25	3-12	<2 nm	1.1	43-45	1.1
4966-96-1	24	10-90	3-7 nm	0.50	0-2	2-2.2

Both catalysts were compared under the same test conditions and at approximate the same CO conversion level of 15%, but at different times on stream. The highly dispersed ruthenium Catalyst 4966-72 showed 43-45% selectivity to CO_2, while Catalyst 4966-96-1 with 3-7 nm ruthenium particles showed virtually no CO production at 208°C. The same table also summarizes the H_2:CO usage ratio for both catalysts. The usage ratio was lower than 2 with Catalyst 4966-72 with high CO_2 selectivity.

At 225°C, Catalyst 4966-72 also showed high selectivity to CO_2 in Run 32 (Figure 5-131) while Catalyst 4966-96-1 showed virtually no selectivity to CO_2 in Run 33 (Figure 5-180). However, the selectivity to CO_2 for the highly dispersed Catalyst 4966-72 was less stable at 225°C relative to the selectivity at 208°C.

Water gas shift reaction during Fischer-Tropsch synthesis with alumina-supported catalysts was apparently catalyzed by highly dispersed ruthenium, and essentially not with larger ruthenium particles. Based on the water gas shift reaction mechanism discussed in Section 2.2.1.4.2, it may be postulated that part of the highly dispersed ruthenium may be in a positive oxidation state during Fischer-Tropsch synthesis.

The observed decrease in selectivity apparent to the water gas shift reaction with time may be explained by agglomeration of highly dispersed ruthenium during the test. The more rapid loss in CO_2 selectiviy at higher

temperatures may be explained by faster ruthenium agglomeration. A short-lived apparent water gas shift activity with catalysts containing larger ruthenium particles may be explained by the presence of a small fraction of highly dispersed ruthenium which rapidly agglomerates.

It is important to note that the water gas shift reaction, like the ruthenium carbonyl formation reaction, probably does not require CO dissociation; that may be why it is favored over smaller ruthenium particles which cannot dissociate CO as effectively as larger particles.

5.2.5.2.2 Olefin-to-Paraffin Ratio

Catalysts 4956-86 (Run 16), 4956-101 (Run 17) and 4956-76 (Run 15) are compared in Figure 5-258. Here, the propylene to propane ratio is plotted versus time on stream. During these tests, the H_2:CO usage ratio was higher than the H_2:CO feed ratio, and accordingly the H_2:CO ratios decreased with increase in conversion level. However, as the catalysts deactivated the conversion levels decreased, and the H_2:CO ratio in the catalyst beds became closer to the feed ratio.

The highest propylene:propane ratio was obtained with Catalyst 4956-76 which contained 4-6 nm ruthenium particles. The propylene:propane ratio decreased slightly from 1.6 to 1.3-1.4 during the first 75 hours in the test possibly because of an increase in the H_2:CO ratio at the reactor outlet from 0.2 to 0.7. After 75 hours, the propylene:propane ration remained nearly constant.

The lowest propylene:propane ratio was obtained with Catalyst 4956-86 which had the smallest ruthenium particle size, less than 2 nm. The propylene: propane ratio increased from 0 to 1.3 during the first 100 hours of the test with highly dispersed ruthenium Catalyst 4956-86, although the H_2:CO ratio at the reactor outlet only slightly decreased from 0.9 to 0.8. The increase in the

Figure 5-258. Propylene:Propane Ratios with Catalysts Having Different Size Ruthenium Particles in Runs 16, 17 and 15 (H_2:CO Feed Ratio = 0.9, 208°C at Inlet, 35 atm)

	Catalyst	Run	H_2:Ru	Ru, nm (STEM)
□	4956-86	16	0.85	<2
○	4956-101	17	0.59	≤2-4
△	4956-76	15	0.29	4-6

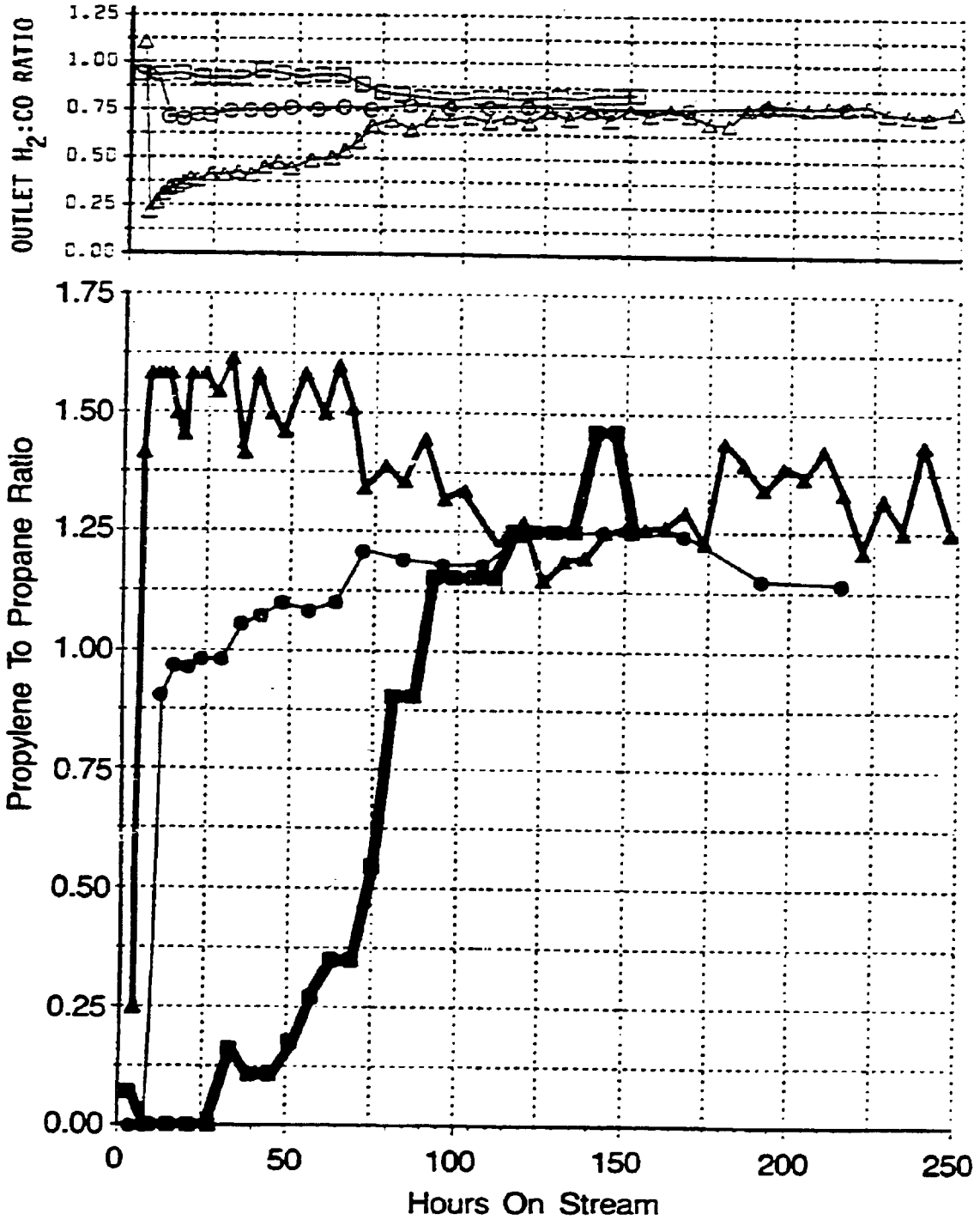

propylene-to-propane ratio with Catalyst 4956-86 occurred concurrently with a decrease in the selectivity to CO_2. Catalyst 4956-101 with intermediate-sized ruthenium particles, showed an intermediate olefin:paraffin ratio between Catalyst 4956-76 and 4956-86.

Butylene:butane ratios showed similar trends to propylene:propane ratios; however, the differences between Catalysts 4956-86, 4956-101 and 4956-76 were smaller.

The olefin:paraffin ratios and the test conditions for Catalysts 4966-72, 4966-96-1 and 4966-119 are summarized in Table 5-45.

At 208°C in Run 25, the highly dispersed ruthenium Catalyst 4966-72 did not initially make olefinic products, but there was a slight increase in olefinic product formation during the course of the 12-hour test at constant CO conversion and constant CO_2 selectivity. However, even at the end of the test, the olefin to paraffin ratios were significantly lower with Catalyst 4966-72 which also showed high selectivity for CO_2 production relative to Catalyst 4966-96-1 with 3-7 nm ruthenium particles in Run 24.

Catalyst 4966-72 was also evaluated in Run 32 at 225°C and compared to Catalyst 4966-96-1 in Run 33 after Catalyst 4966-72's selectivity to CO_2 decreased during the test to a very low value. In the absence of any substantial H_2 production through the water gas shift reaction, at 22-24% $CO+H_2$ conversion, the propylene:propane ratio was only slightly lower or comparable with Catalyst 4966-72 relative to Catalyst 4966-96-1, while the butylene:butane ratio was the same for both catalysts. At 64-66% $CO+H_2$ conversion, Catalyst 4966-72 was compared to Catalyst 4966-119 tested in Run 34, which had similar average size ruthenium particle sizes as Catalyst 4966-96-1. The propylene:propane ratio was significantly higher with Catalyst 4966-119, while the butylene:butane ratio may have been slightly higher relative to Catalyst 4966-72.

Table 5-45

Variation of Olefin to Paraffin Ratio with Ruthenium Catalysts Having Different Ruthenium Particle Sizes on Alumina
H_2:CO Ratio = 2.0±0.1; 35 atm

Catalyst	Initial Ru Particle Size	H_2:Ru	Run	Hours on Stream	Inlet T, °C	GHSV	$CO+H_2$ Conversion, %	CO_2 Selectivity, %	Olefin:Paraffin C_3	Olefin:Paraffin C_4	Maximum T, °C
4966-72	<2 nm	1.1	25	3-12	208	140	10	43-45	0+0.1	0+0.2	210-211
			32	28-30	225	320	22	2	1.1	1.1	228
			32	25-28	225	65	63-64	2	1.2	1.1	232
4966-96-1	3-7 nm	0.5	24	23-50	208	125-250	6-17	1	1.3	1.0	210
			33	18-24	225	390	24	1	1.8	1.1	231
4966-119	4-6 nm		34	40-50	225	170	66	2	2.0	1.3	232

In situ production of H_2 through the water gas shift reaction is partly responsible for the low selectivity to olefinic products observed with the highly dispersed ruthenium catalysts. In the absence of any significant water gas shift activity, the propylene:propane ratios were still lower with smaller ruthenium particles, while butylene:butane ratios were not significantly different.

It is difficult to compare olefin to paraffin ratios at the same conversion level with catalysts having different activities because of the use of different space velocities which may, in turn, influence the olefin to paraffin ratios. Accordingly, it is not possible to draw definite conclusions about the effect of ruthenium particle size on the olefin:paraffin ratios.

The increase in the olefin:paraffin ratio during the test at constant conversion and CO_2 selectivity with a highly dispersed ruthenium catalyst may be explained by ruthenium metal agglomeration. This ruthenium agglomeration during the test may minimize olefin:paraffin ratio differences observed between catalysts.

5.2.5.2.3 Chain Growth Probability

For all ruthenium catalysts evaluated in this work, product distributions obeyed the Anderson-Schulz-Flory polymerization law with a higher chain growth probability α_2 between carbon numbers 20 to 150-200, and a lower chain growth probability α_1 at lower carbon numbers. The C_2-C_3 hydrocarbons always showed negative deviations from the Anderson-Schulz-Flory line at carbon numbers less than 20, with the largest deviations at C_2 and the smallest deviations at C_4. Nevertheless, C_1-C_4 light ends selectivity always varied inversely both with α_1 and α_2.

Catalysts 4956-86, 4956-101 and 4956-76 were tested at 208°C and $0.9H_2$:1CO feed ratio and it was determined that, under these conditions, the light ends selectivity was relatively insensitive to the conversion level. Catalysts 4966-72 and 4966-96-1 were tested at 225°C (or 208°C) and $2H_2$:1CO feed ratio and it was determined that, under those conditions, the light ends selectivity increased with a decrease in the conversion level when the conversion was decreased by increasing the space velocity or through deactivation.

The light ends selectivity obtained with Catalysts 4956-86 (Run 16), 4956-101 (Run 17) and 4956-76 (Run 15) at 18% $CO+H_2$ conversion and Catalysts 4966-72 in Run 32 and 4966-96-1 in Run 33 at 14-69% conversion are summarized as a function of the H_2:Ru ratio in Table 5-46. In the case of highly dispersed Catalysts 4966-72 and 4956-86, the light ends selectivities were calculated at times on stream when the H_2 production through the water gas shift reaction was significantly low ($\leq$9% selectivity to CO_2).

The light ends selectivities were calculated in the following manner:

$$\text{Selectivity to } C_n = \frac{(C_n/Ar)_{product}}{(\frac{CO}{Ar})_{feed} - (\frac{CO}{Ar})_{product} - (\frac{CO_2}{Ar})_{product}}$$

$$\text{Light ends selectivities} = \sum_{n=1}^{4} \text{selectivity to } C_n.$$

It was determined that, even at constant CO conversion and constant CO_2 selectivity, the light ends selectivity decreased during the test with a highly dispersed catalyst, apparently because of ruthenium agglomeration (Figure 5-259). Accordingly, the light ends selectivities that were measured for these catalysts present a lower bound to the intrinsic light ends selectivities.

Table 5-46

Variation of Light Ends Selectivity with Ruthenium Particle Size on Alumina

All tests at 34 atm

Catalyst	H_2:Ru	T, °C (Inlet)	Run	Hours on Stream	H_2:CO (Average in Catalyst Bed)	$CO+H_2$ Conversion %	CO_2 Selectivity %	C_1-C_4* Selectivity %
4956-86	0.85	208	16	80-85	0.8-0.9	18	9	4.8
4956-101	0.59	208	17	50-60	0.8-0.9	18	1	2.2
4956-76	0.29	208	15	155-170	0.8-0.9	18	0	1.4
4966-72	1.1	225	32	11-14	2.0	15	2	13
				20-22	2.0	50-52	2	8.1
				25-27	2.1	62-64	2	8.3
4966-96-1	0.50	225	33	25-28	1.9	16	1	9.2
				12	1.8-1.9	50	1	6.4
				10	1.7-1.8	69	1	5.9

*CO_2 selectivity normalized out.

The results summarized in Table 5-46 and Figure 5-259 clearly illustrate that C_1-C_4 light ends selectivity increases (or the chain growth probability decreases) with an increase in the H_2:Ru ratio or with a decrease in the ruthenium metal particle size.

Chain growth probability, like the turnover frequency for hydrocarbon synthesis, increased with an increase in ruthenium particle size, which is consistent with what was observed by Kellner and Bell [55] and Fukushima, *et al.* [56]. Concurrent increase in chain growth probability and turnover frequency with increase in ruthenium particle size may be explained if the overall rate is controlled either by CO dissociation or by chain growth, both of which are likely to require a large ensemble of atoms.

The Anderson-Schulz-Flory distributions obtained with Catalyst 4956-86 in the form of highly dispersed ruthenium (<2 nm particles) and with Catalyst 4956-76 in the form of 4-6 nm ruthenium particles in Runs 16 and 15 respectively, at 0.9H_2:CO feed ratio, 208°C at inlet and 35 atm are illustrated in Figures 5-260 amd 5-261. The chain growth probability (α) was higher for the entire carbon number range in Run 15. Although the test conditions were the same, the higher conversion level achieved with the more active catalyst in the form of 4-6 nm ruthenium particles in Run 15 caused the H_2:CO ratio at the reactor outlet to be lower and therefore partly responsible for the higher chain growth probability that was observed.

In an attempt to remove the H_2:CO ratio effect from the ruthenium particle size effect in Figure 5-262, the Anderson-Schulz-Flory distributions obtained with two highly dispersed ruthenium Catalysts 4956-86 and 4966-72 tested at H_2:CO feed ratios of 0.9 and 3.0 in Runs 16 ands 18 were compared in Figures 5-262 and 5-263. Other test conditions were the same in both runs. The

Figure 5-259

EFFECT OF Ru PARTICLE SIZE ON LIGHT ENDS PRODUCTION HIGH H_2:CO RATIO DATA

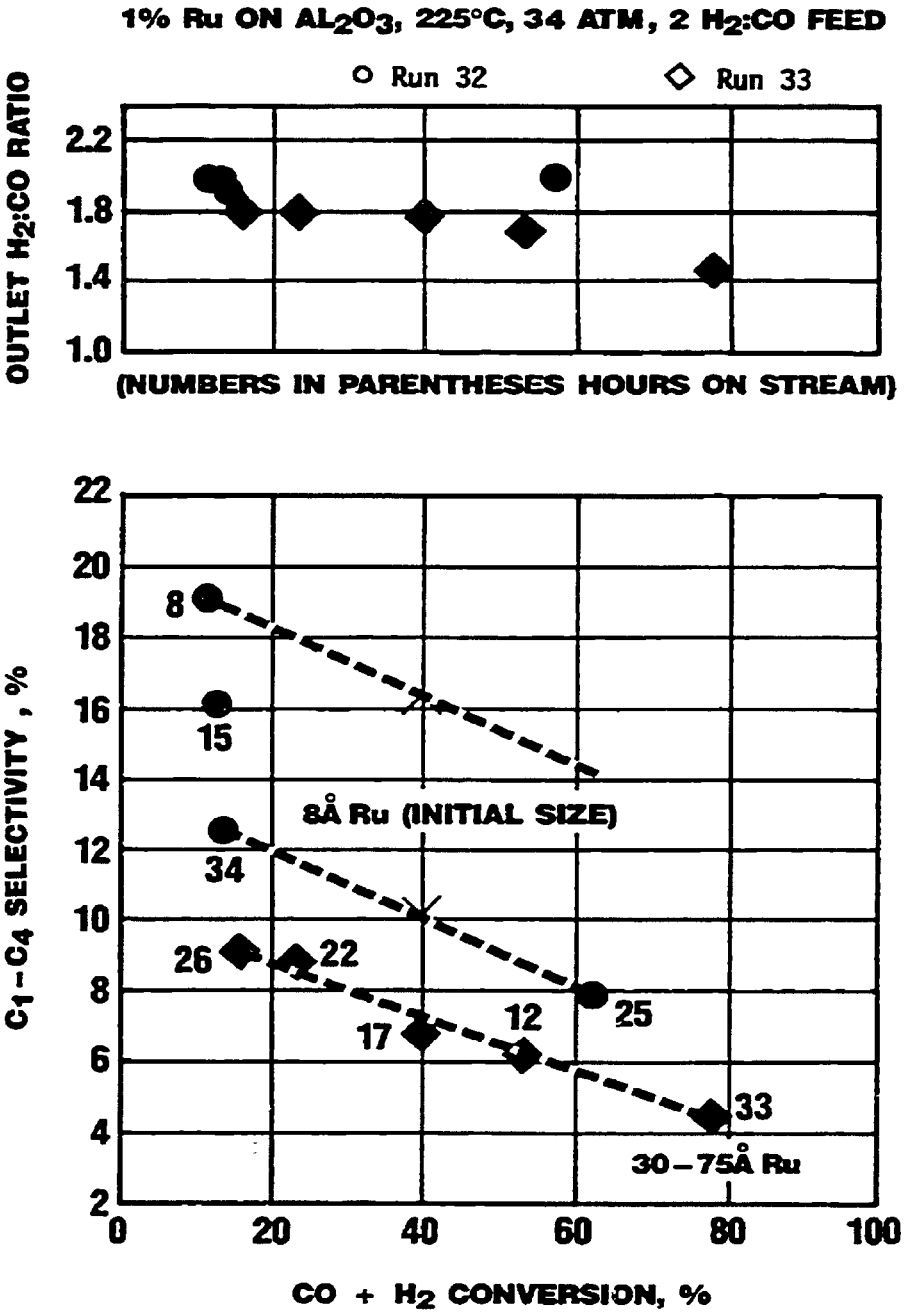

Figure 5-260

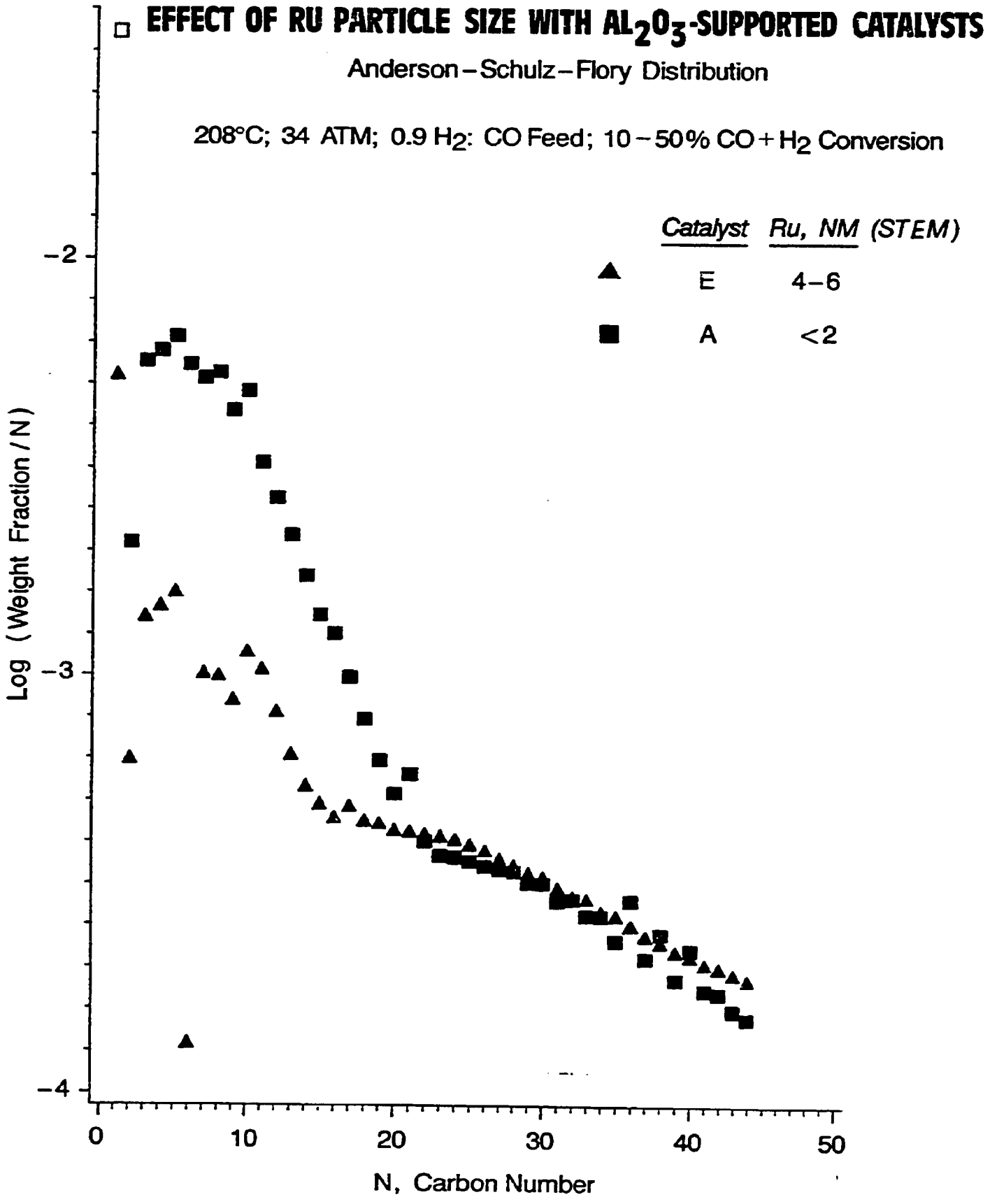
EFFECT OF RU PARTICLE SIZE WITH AL_2O_3-SUPPORTED CATALYSTS
Anderson–Schulz–Flory Distribution
208°C; 34 ATM; 0.9 H_2: CO Feed; 10–50% CO + H_2 Conversion
Catalyst Ru, NM (STEM)
E 4–6
A <2
Log (Weight Fraction / N)
−2
−3
−4
0
10
20
30
40
50
N, Carbon Number

Figure 5-261

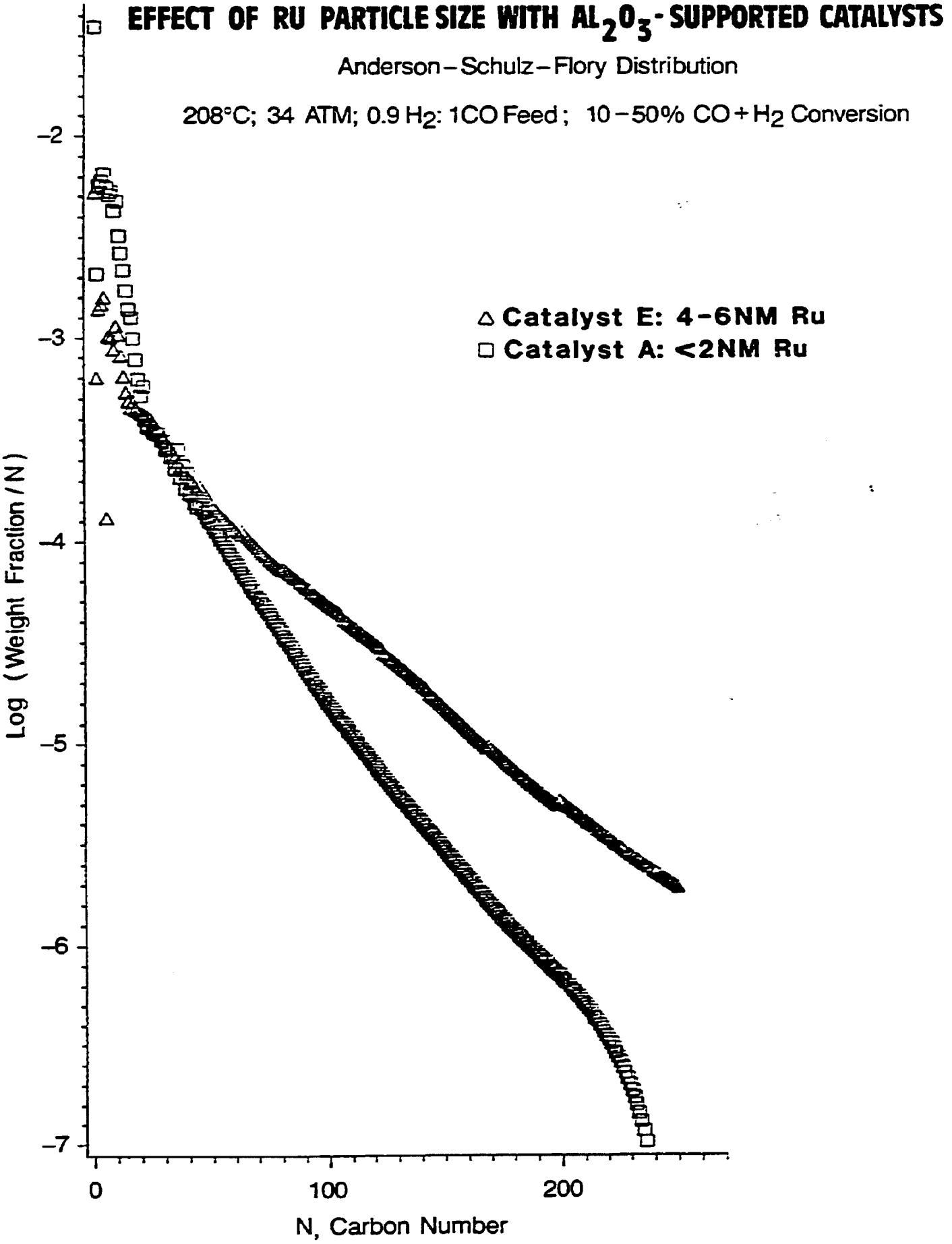
EFFECT OF RU PARTICLE SIZE WITH AL_2O_3-SUPPORTED CATALYSTS
Anderson–Schulz–Flory Distribution
208°C; 34 ATM; 0.9 H_2: 1CO Feed; 10–50% CO + H_2 Conversion
△ Catalyst E: 4–6NM Ru
□ Catalyst A: <2NM Ru
Log (Weight Fraction / N)
-2
-3
-4
-5
-6
-7
0
100
200
N, Carbon Number

Figure 5-262. Anderson-Schulz-Flory Distributions in Runs 16 and 18 with Highly Dispersed Ruthenium Catalysts 4956-86 and 4966-72 (Hydrocarbons only; C_1-C_{44})

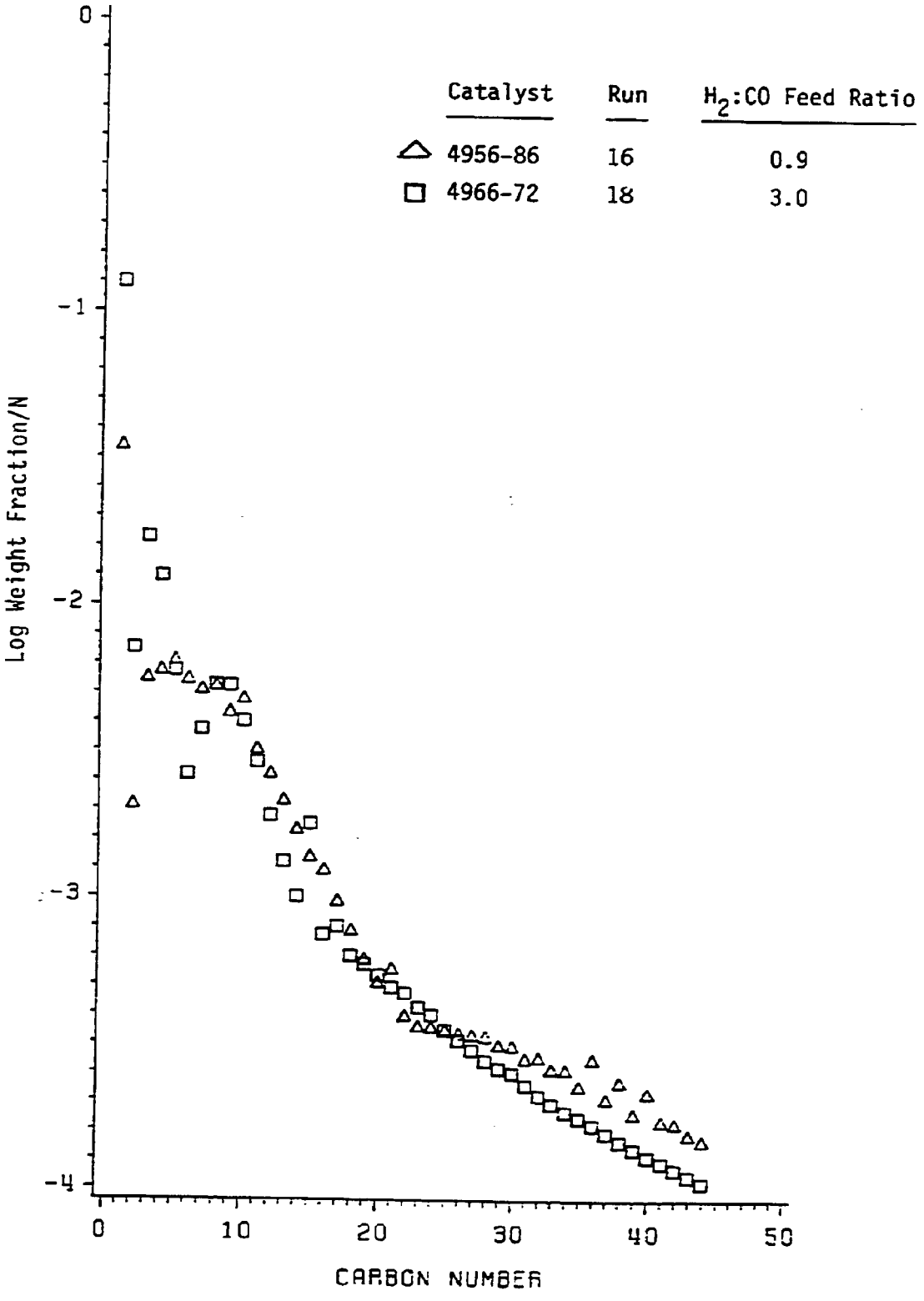

Figure 5-263. Anderson-Schulz-Flory Distributions in Runs 16 and 18 with Highly Dispersed Ruthenium Catalysts 4956-86 and 4966-72 (Hydrocarbons only; C_1-C_{250})

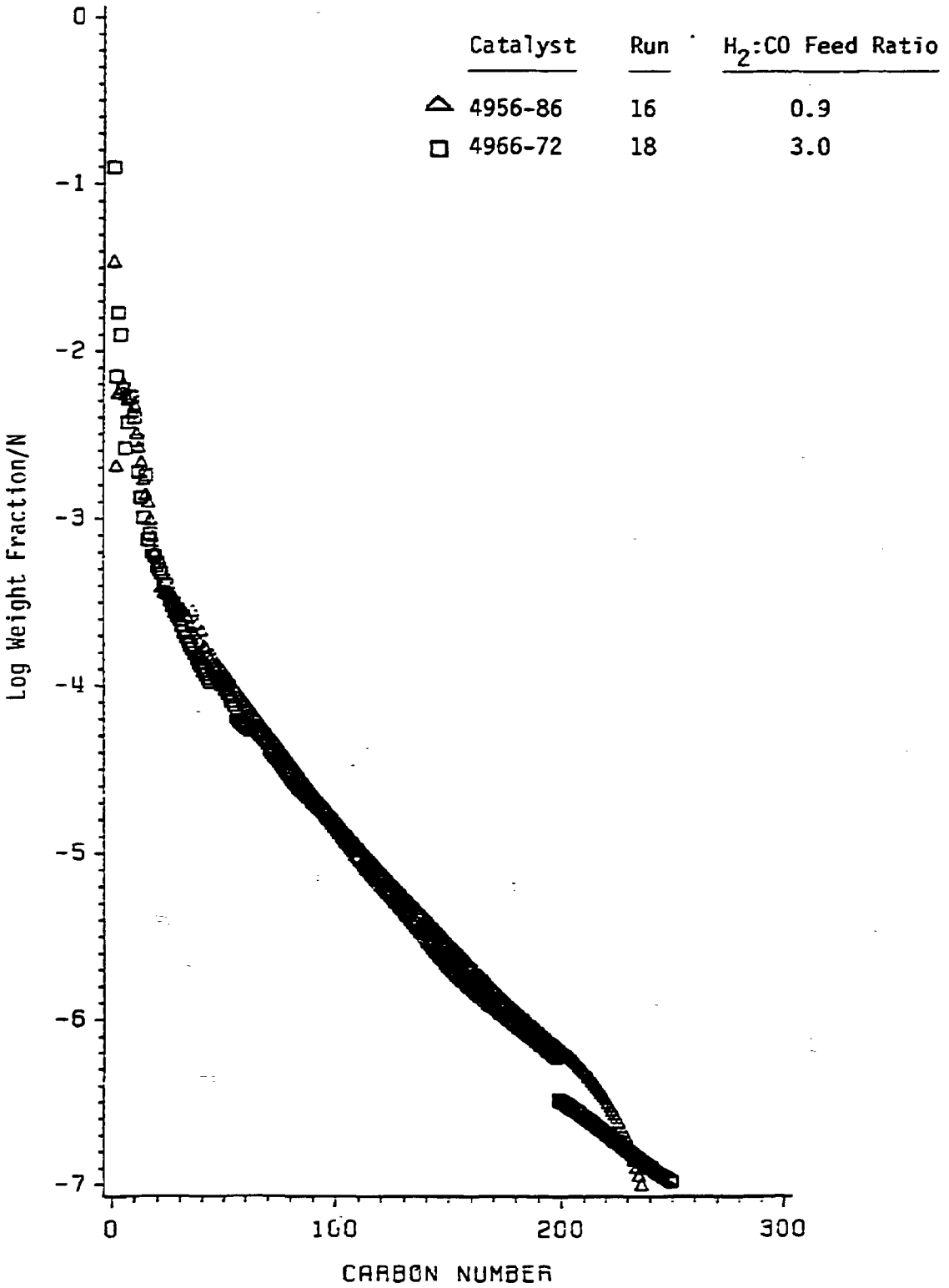

comparison in Figure 5-263 shows that, apparently, the lower H_2:CO ratio in R 18 lowered the selectivities to light ends in the C_1-C_{18} carbon number range while causing only a minor change in the product selectivities at higher carb numbers. These results suggest that the selectivity differences in the entir carbon number range illustrated in Figure 5-261 are mostly caused by ruthenium particle size effects and not by H_2:CO ratio effects.

5.2.6 Support Effects on Ruthenium Catalytic Performance in Fischer-Tropsch Synthesis

There are not enough data in this work to reach conclusions about the effect of support on the catalytic performance of ruthenium in Fischer-Tropsch synthesis. Nevertheless, the available data were compiled in Table 5-47 in an attempt to summarize some of the observations.

5.2.6.1 Y-Zeolite vs. Al_2O_3

The significance of Y-zeolite vs. alumina support in ruthenium catalyst performance was investigated by comparing the performance of Catalysts 4966-114 (6.3% Ru on Y-zeolite) and 4966-76 (0.84% Ru on Al_2O_3). The ruthenium compound that were used and the preparation procedures were different with these two catalysts (Table 5-41). Nevertheless, similar ruthenium particle sizes of abou 1.5 nm were obtained, except for the presence of some 2-4 nm particles in the alumina-supported catalyst. Catalysts 4966-114 and 4966-76 were tested at H_2:C feed ratio = 1.5, 200°C at inlet and 15 atm in Runs 28 and 20, respectively. I was previously discussed that ruthenium agglomerated on alumina but not on Y-zeolite in these tests.

The Y-zeolite-supported catalyst showed 28% CO conversion at 1248 gas hourly space velocity at 5 hours on stream, while the alumina-supported catalyst showed 20% CO conversion at 50 hr^{-1} after 6 hours on stream. These give the initial activity in moles CO converted/sec-mole ruthenium 0.0061 for the Y-zeolite-supported catalyst and 0.0021 for the alumina-supported catalyst.

The selectivities of these two catalysts were compared at 20% $CO+H_2$ conversion. Selectivities to methane and to other light hydrocarbons were significantly higher with the Y-zeolite-supported catalyst. The run-average Anderson-Schulz-Flory distributions also indicate lower chain growth probabilities in Run 28 with Y-zeolite-supported catalyst (Figure 5-264).

There was essentially no olefin formation at carbon number 3 and 4 with the alumina-supported catalyst. The olefin to paraffin ratios were much higher with the Y-zeolite-supported catalyst. It is conceivable that some of the differences in the olefin to paraffin ratios observed between these two catalysts is attributed to the *in situ* generation of H_2 via the water gas shift reaction with the alumina-supported catalyst. The water gas shift activity for the Y-zeolite support catalyst was nil.

Figure 5-264

RUTHENIUM CATALYSTS PREPARED ON DIFFERENT SUPPORTS
ANDERSON-SCHULZ-FLORY DISTRIBUTIONS